Steady-State Empirical Model for Electrical Activation of Silicon-Implanted Gallium Nitride

Alexander Toifl
Institute for Microelectronics
TU Wien
Wien, Austria
toifl@iue.tuwien.ac.at

Vito Šimonka
Christian Doppler Laboratory
for High Performance TCAD
Institute for Microelectronics, TU Wien
Wien, Austria
simonka@iue.tuwien.ac.at

Andreas Hössinger
Silvaco Europe Ltd.
Cambridge, United Kingdom
andreas.hoessinger@silvaco.com

Siegfried Selberherr
Institute for Microelectronics
TU Wien
Wien, Austria
selberherr@iue.tuwien.ac.at

Josef Weinbub
Christian Doppler Laboratory
for High Performance TCAD
Institute for Microelectronics, TU Wien
Wien, Austria
weinbub@iue.tuwien.ac.at

***Abstract*—We propose a steady-state empirical activation model for the prediction of the electrical activation efficiency of silicon-implanted gallium nitride. Our model has been implemented into Silvaco's Victory Process simulator which we utilize to perform an accurate prediction of the dopant activation profiles. The dopant activation strongly influences the device characteristics, which is demonstrated by device simulations of a state-of-the-art junction barrier Schottky rectifier. Our results show that increasing the annealing temperature by fifty degrees Celsius reduces the device's on-state resistance by one order of magnitude.**

***Index Terms*—Gallium nitride, implantation, annealing, electrical activation, power devices, modeling**

I. Introduction

Gallium nitride (GaN) is highly attractive for power electronic devices, due to its excellent material properties, in particular its wide bandgap ($3.4\,\mathrm{eV}$) [1]. Even though GaN based devices which employ horizontal current flow have been successfully investigated [2], GaN exhibits exceptional figure-of-merits for vertical power devices (e.g., Schottky diodes, current aperture vertical electron transistors, and heterostructure field-effect transistors). As discussed by Baliga [3] GaN's on-resistance based figure-of merit exceeds the value of the predominant wide bandgap semiconductor silicon carbide (SiC).

The majority of vertical GaN power device structures requires doping by an ion implantation process with a subsequent thermal annealing step [1], [4]. The annealing step repairs the lattice damage introduced by the ion bombardment and provides the required energy for the implanted dopants to occupy lattice sites. A well-controlled annealing process is thus essential for the electrical activation of the implanted dopants. Therefore, implantation and annealing are critical fabrications steps, ultimately defining electrical properties of the devices.

For GaN the annealing process is significantly more challenging compared to elemental or other compound semiconductors (e.g., SiC) [5]. Due to the high melting point of GaN ($2500\,^{\circ}\mathrm{C}$), annealing temperatures ranging from $1000\,^{\circ}\mathrm{C}$ to $1400\,^{\circ}\mathrm{C}$ are required. However, GaN starts to decompose at significantly lower temperatures ($\approx 840\,^{\circ}\mathrm{C}$), which causes the need for protective caps and limits the maximum annealing times ($<10\,\mathrm{min}$) [6], [7]. Even though the activation mechanisms are not fully understood (in particular for acceptor-type dopants), several groups have successfully achieved highly efficient electrical activation of silicon (Si)-implanted GaN (n-type doping) [8] [9], [10], [11]. Strikingly, a reduced activation efficiency for low ($\approx 10^{17}\,\mathrm{cm}^{-3}$) and moderate ($\approx 10^{18}\,\mathrm{cm}^{-3}$) doping concentrations has been observed [8], [9], [10], which is in contrast to the full activation which is typically achieved in other semiconductors like SiC [12]. This phenomenon has been attributed to compensation by unintentionally introduced elements such as carbon, but is still controversially discussed in the literature [10], [13], [14].

In this work we propose an empirical model which accounts for the reduction of the activation efficiency at low implanted concentrations. We concentrate on the accurate description of the electrical activation efficiency with regard to the main annealing process parameters, i.e., annealing temperature and implanted dopant concentration. The proposed model has been implemented into Silvaco's Victory Process simulator [15] which we utilize to investigate the impact of the activation efficiency on the device characteristics of a state-of-the-art Si-implanted GaN junction barrier Schottky (JBS) rectifier.

978-1-5386-6790-3/18/$31.00 ©2018 IEEE

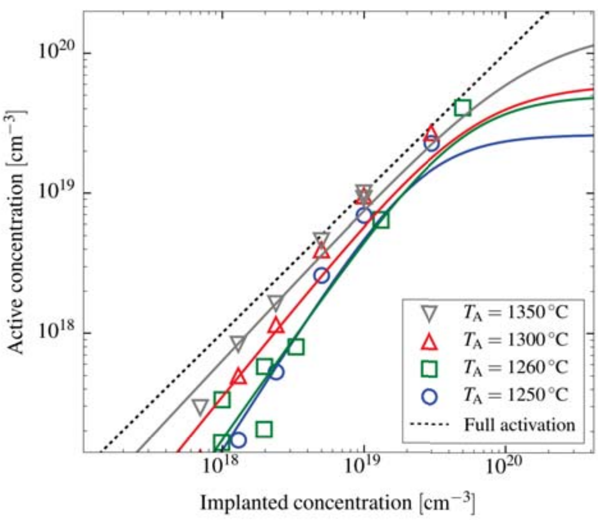

Fig. 1. Electrically active concentration $C_{\rm a}$ for Si-implanted GaN as a function of implanted concentration $C_{\rm x}$ for various annealing temperatures $T_{\rm A}$. The figure shows the fit of the proposed model (1) (solid lines) to the experimental data [8], [9], [10], [11] (open symbols). The model is capable of describing the reduced activation for low implanted dopant concentrations.

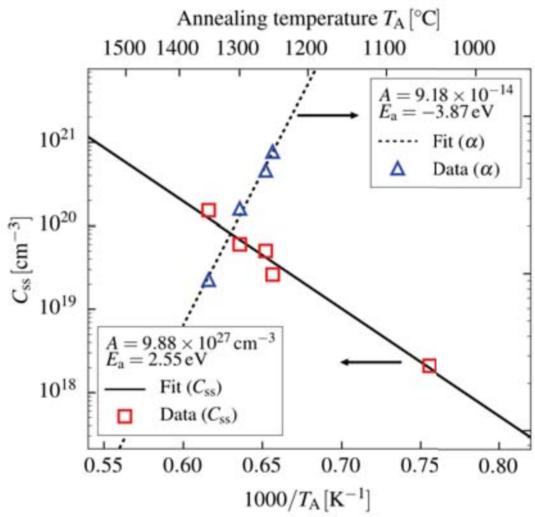

Fig. 2. The model parameters $C_{\rm ss}$ and α as a function of annealing temperature $T_{\rm A}$. The parameter values (open symbols) are obtained from the proposed model (1) and are fitted with the Arrhenius equation (3).

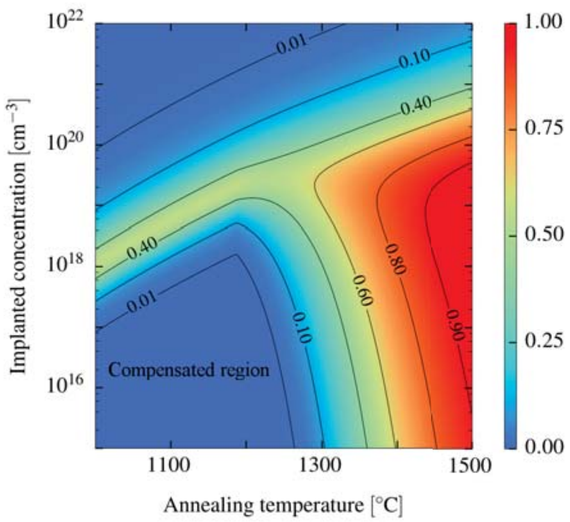

Fig. 3. Activation efficiency as a function of annealing temperature and implanted concentration. The proposed model (1) predicts reduced electrical activation for low implanted concentrations and annealing temperatures.

II. Activation Model

We propose a steady-state empirical model for the electrical activation of dopants after implantation into GaN. The model extends our activation model which has already been successfully employed for aluminium and phosphorus-implanted SiC [16]. The active dopant concentration $C_{\rm a}$ is expressed as a function of the annealing temperature $T_{\rm A}$ and implanted dopant concentration $C_{\rm x}$ such that

$$C_{\rm a}(T_{\rm A}, C_{\rm x}) = \frac{C_{\rm x}\,F}{1+\frac{C_{\rm x}\,F}{C_{\rm ss}(T_{\rm A})}} \tag{1}$$

with the empirical factor

$$F = \left(\frac{C_{\rm x}}{C_{\rm ss}(T_{\rm A})}\right)^{\alpha(T_{\rm A})}. \tag{2}$$

α is an empirical exponent, typically in the range of 0 to 2, related to the concentration of compensating species. $C_{\rm ss}$ governs the maximum achievable active concentration and is related to the solid solubility of the dopants in GaN. Both parameters $C_{\rm ss}$ and α follow an Arrhenius law

$$Q = A\,\exp\left(-\frac{E_{\rm a}}{k_{\rm B}T_{\rm A}}\right), \quad Q = C_{\rm ss} \text{ or } \alpha \tag{3}$$

with a prefactor A, the Boltzmann constant $k_{\rm B}$, and activation energy $E_{\rm a}$. The proposed activation model provides the capabilities to predict the activation efficiency

$$R_{\rm act} = \frac{C_{\rm a}}{C_{\rm x}}. \tag{4}$$

For the fabrication of state-of-the-art devices a high activation efficiency is essential. It can be well predicted with the proposed model, which allows to optimize the implantation and annealing process parameters.

III. Method

The proposed model is calibrated according to publicly available experimental data for Si-implanted GaN, assuming that the employed capping technique (e.g., aluminum nitride or silicon oxide caps) does not influence the activation efficiency [8], [9], [10], [11]. This assumption is required due to the low amount of data available for model fitting.

The fitting curves are shown in Fig. 1. The associated model parameters are confirmed to follow the Arrhenius law, as shown in Fig. 2. The experimental data set has been fitted with very high accuracy, particularly in the critical region

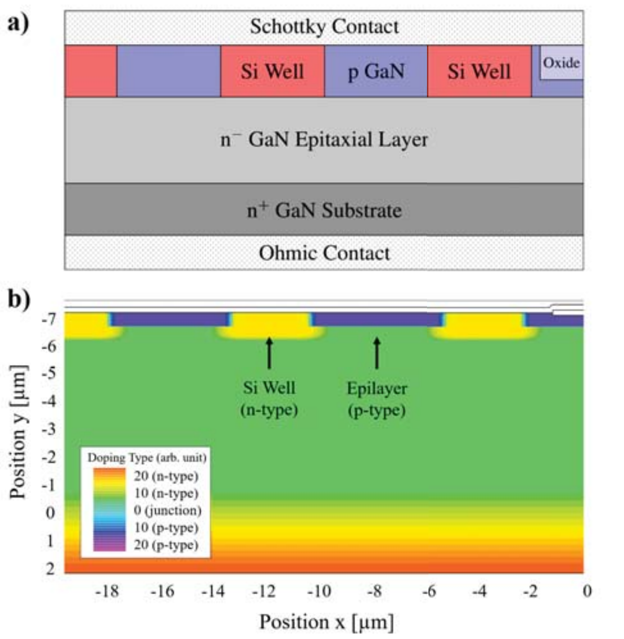

Fig. 4. **a)** The schematic cross section of the considered GaN JBS rectifier is characterized by periodic Si wells, which are fabricated with ion implantation. **b)** Final device structure of the considered JBS rectifier, which originates from the process simulation and is further used for device simulations.

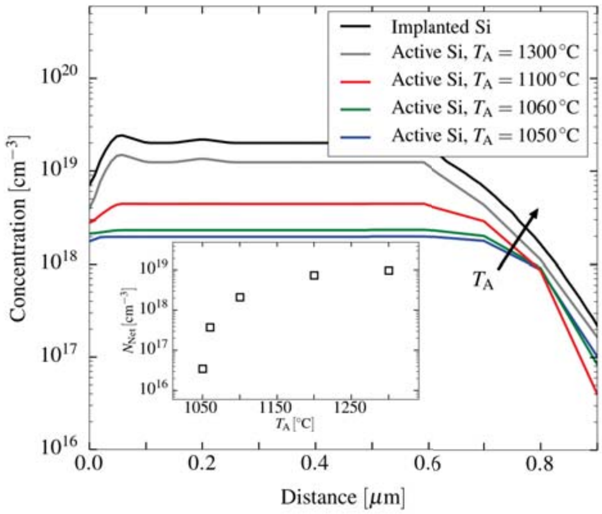

Fig. 5. Doping over depth profiles for the Si-implanted wells of the GaN JBS rectifiers. Elevated annealing temperatures T_{A} enhance the activation of Si and thus increase the net doping concentration N_{Net}, as shown in the inset figure.

of the reduced activation efficiency for low concentrations. The parameter estimation procedure employs the least squares method for which the average numerical fitting error is $<8\,\%$.

Additionally, we have evaluated the calibrated activation model (1). Fig. 3 shows a phase diagram of the activation efficiency as a function of annealing temperature and implanted dopant concentration. For low dopant concentration ($<10^{17}\,\mathrm{cm}^{-3}$) a phase region with reduced activation (compensated region) is observed in agreement with the experimental results.

In order to demonstrate the model's capabilities, process and device simulations of Si-implanted GaN JBS rectifiers - as recently presented by Zhang *et al.* [17] - have been conducted. The coupled simulations approach allows to investigate the impact of the process parameters, i.e., implanted dopant concentration and annealing temperature, on the device characteristics.

The fabrication process is simulated by closely following the steps presented by Zhang *et al*. [17] Starting with a highly n-doped (0001) GaN substrate, n-doped ($7\,\mu\mathrm{m}$), and p-doped epitaxial layers ($0.5\,\mu\mathrm{m}$) are grown. The deposition and selective etching of an implantation mask (silicon oxide $\mathrm{SiO_2}$) enables to selectively implant Si into the layers, forming a regular grid of implanted Si wells, which locally converts the p-doped epilayer to conductive n-type channels. The resulting n-type and p-type regions have both a nominal width of $3\,\mu\mathrm{m}$. The annealing step is simulated employing the calibrated activation model. During the annealing process the surface is protected with a $\mathrm{SiO_2}$ cap. Finally the etching, oxidation (edge termination), and metal deposition process steps are simulated. The schematic cross section and the resulting JBS rectifier structure are shown in Fig. 4.

In order to investigate the impact of the annealing process parameters on the actual device characteristics, device simulations for the fabricated JBS rectifiers are performed using Silvaco's Victory Device simulator [15]. For the device simulations the drift-diffusion equations are solved at room temperature. GaN's carrier-transport related properties are incorporated by modeling incomplete ionization, Shockley-Read-Hall and Auger recombination, and bandgap and carrier mobility with the expressions and parameters presented by Sabui *et al*. [18]. Additionally, the 'GaNsat High-Field Mobility Model' proposed by Farahmand *et al.* [19] is employed. For the ohmic contact fixed potential Dirichlet boundary conditions are employed and the Schottky contact is modeled using a workfunction-based model with a workfunction $E_{\mathrm{w}} = 5.25\,\mathrm{eV}$.

IV. Simulation Results and Discussion

The doping over depth profiles for the Si wells as obtained by process simulation are shown in Fig. 5. For an annealing temperature $T_{\mathrm{A}} = 1050\,°\mathrm{C}$ employed by Zhang *et al.* [17], the model gives a mean net doping concentration $N_{\mathrm{Net}} = 5 \times 10^{16}\,\mathrm{cm}^{-3}$, which is consistent with experimental observations. Elevated annealing temperatures ($T_{\mathrm{A}} = 1060$, 1100, and $1300\,°\mathrm{C}$) promote the annealing process and a significant improvement of the activation efficiency can be obtained. In particular, the net doping concentration is increased up to three orders of magnitude, shown in the inset of Fig. 5.

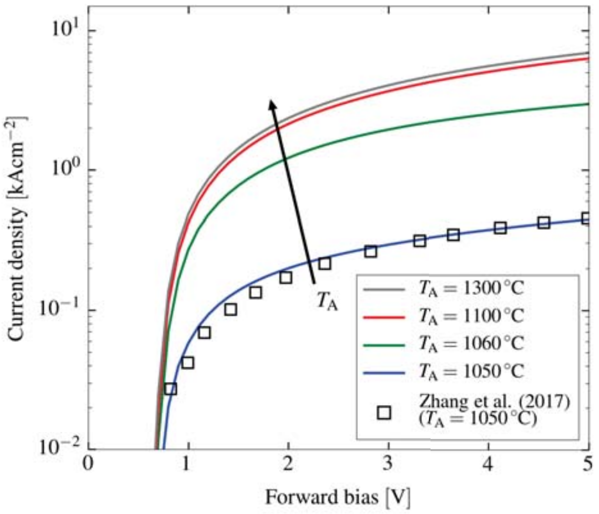

Fig. 6. The forward I-V characteristics of the GaN JBS rectifiers presented by Zhang *et al.* [17] is accurately reproduced using the proposed model (1). It is evident that the annealing temperature T_A strongly affects the forward current density J_D and the on-resistance R_on.

Our device simulation results accurately reproduce the forward voltage $V_\mathrm{on} = 0.7\,\mathrm{V}$ and the specific on-state resistance $R_\mathrm{on} = 7.6\,\mathrm{m\Omega\,cm^{-2}}$ as reported by Zhang *et al.* [17]. In addition, Fig. 6 shows the strong impact of the annealing temperature on the device operation. Increasing the annealing temperature to $1100\,°\mathrm{C}$ results in a specific on-resistance $R_\mathrm{on} = 0.58\,\mathrm{m\Omega\,cm^{-2}}$, indicating an improvement in the range of one order of magnitude.

V. Conclusions

We have proposed an empirical electrical activation model for Si-implanted GaN that accurately characterizes the steady-state active dopant concentration with respect to the annealing temperature and implanted dopant concentration. The model provides the capabilities to describe the reduced activation for low dopant concentrations and has been validated by comparing the predictions with experimental data.

The activation model was implemented into Victory Process simulator, which allowed us to set up closely coupled process and device simulations. A state-of-the-art JBS rectifier was investigated, which requires a high quality annealing step for local conversion of a p-doped epitaxial layer to n-doped wells. The doping depth profiles are strongly influenced by the annealing temperature. Elevating the annealing temperature from $1050\,°\mathrm{C}$ to $1300\,°\mathrm{C}$ was found to enhance the net doping concentration by three orders of magnitude.

With the coupled process and device simulations we were able to investigate the impact of the process parameters on the actual device characteristics. Elevated annealing temperatures were confirmed to significantly raise the forward diode current which lead to a reduction of the on-resistance by one order of magnitude.

Our results corroborate the high relevance of the modeling capabilities of implantation and annealing fabrication steps.

Acknowledgment

The financial support by the *Austrian Federal Ministry for Digital and Economic Affairs* and the *National Foundation for Research, Technology and Development* is gratefully acknowledged.

References

[1] T. J. Flack, B. N. Pushpakaran, and S. B. Bayne, "GaN Technology for Power Electronic Applications: A Review," *J. Electron. Mater.*, vol. 45, no. 6, pp. 2673–2682, 2016.

[2] S. Fujita, "Wide-bandgap Semiconductor Materials: For their full Bloom," *Jpn. J. Appl. Phys.*, vol. 54, no. 3, p. 030101, 2015.

[3] B. J. Baliga, "Gallium Nitride Devices for Power Electronic Applications," *Semicond. Sci. Tech.*, vol. 28, no. 7, 2013.

[4] K. Nomoto, K. Takahashi, O. Takuya, H. Ogawa, T. Nishimura *et al.*, "Ion Implantation into GaN and Implanted GaN Power Transistors," *ECS Trans.*, vol. 69, pp. 105–112, 2015.

[5] V. Šimonka, A. Hössinger, J. Weinbub, and S. Selberherr, "Empirical Model for Electrical Activation of Aluminium and Boron Doped Silicon Carbide," *IEEE T. Electron. Dev.*, vol. 65, no. 2, pp. 1–6, 2018.

[6] S. Kucheyev, J. Williams, and S. Pearton, "Ion Implantation into GaN," *Mater. Sci. Eng.*, vol. 33, no. 2, pp. 51–108, 2001.

[7] T. J. Anderson, J. D. Greenlee, B. N. Feigelson, J. K. Hite, K. D. Hobart *et al.*, "Improvements in the Annealing of Mg Ion Implanted GaN and related Devices," *IEEE T. Semiconduct. M.*, vol. 29, no. 4, pp. 343–348, 2016.

[8] J. A. Fellows, Y. K. Yeo, R. L. Hengehold, and D. K. Johnstone, "Electrical Activation Studies of GaN Implanted with Si from Low to High Dose," *Appl. Phys. Lett.*, vol. 80, no. 11, pp. 1930–1932, 2002.

[9] Y. Irokawa, O. Fujishima, T. Kachi, and Y. Nakano, "Electrical Activation Characteristics of Silicon-implanted GaN," *J. Appl. Phys.*, vol. 97, no. 8, pp. 1–6, 2005.

[10] Y. Niiyama, S. Ootomo, J. Li, H. Kambayashi, T. Nomura *et al.*, "Si Ion Implantation into Mg-doped GaN for Fabrication of Reduced Surface Field Metal-Oxide-Semiconductor Field-Effect Transistors," *Jpn. J. Appl. Phys.*, vol. 47, no. 7, pp. 5409–5416, 2008.

[11] C. E. Hager, K. A. Jones, M. A. Derenge, and T. S. Zheleva, "Activation of Ion Implanted Si in GaN using a Dual AlN Annealing Cap," *J. Appl. Phys.*, vol. 105, no. 3, p. 033713, 2009.

[12] V. Šimonka, A. Hössinger, J. Weinbub, and S. Selberherr, "Modeling of Electrical Activation Ratios of Phosphorus and Nitrogen Doped Silicon Carbide," in *Proc. Int. Conf. Simulation Semiconductor Processes and Devices (SISPAD)*, 2017, pp. 125–128.

[13] T. Zhu and R. A. Oliver, "Unintentional Doping in GaN," *Phys. Chem. Chem. Phys.*, vol. 14, no. 27, pp. 9558–9573, 2012.

[14] I. C. Kizilyalli, A. P. Edwards, O. Aktas, T. Prunty, and D. Bour, "Vertical Power p-n Diodes Based on Bulk GaN," *IEEE T. Electron. Dev.*, vol. 62, no. 2, pp. 414–422, 2015.

[15] "Silvaco TCAD," https://www.silvaco.com/products/tcad.html, (accessed June 19, 2018).

[16] V. Šimonka, A. Toifl, A. Hössinger, S. Selberherr, and J. Weinbub, "Transient Model for Electrical Activation of Aluminium and Phosphorus-implanted Silicon Carbide," *J. Appl. Phys.*, vol. 123, no. 23, p. 235701, 2018.

[17] Y. Zhang, Z. Liu, M. J. Tadjer, M. Sun, D. Piedra *et al.*, "Vertical GaN Junction Barrier Schottky Rectifiers by Selective Ion Implantation," *IEEE Elec. Dev. Lett.*, vol. 38, no. 8, pp. 1097–1100, 2017.

[18] G. Sabui, P. Parbrook, M. Arredondo-Arechavala, and Z. Shen, "Modeling and Simulation of Bulk Gallium Nitride Power Semiconductor Devices," *AIP Advances*, vol. 6, no. 5, p. 055006, 2016.

[19] M. Farahmand, C. Garetto, E. Bellotti, K. Brennan, M. Goano *et al.*, "Monte Carlo Simulation of Electron Transport in the III-Nitride Wurtzite Phase Materials System: Binaries and Ternaries," *IEEE T. Electron. Dev.*, vol. 48, no. 3, pp. 535–542, 2001.